Identification of the maze in the conformational landscape of fenchol

Elias M Neeman, Thérèse R Huet

Identification of the maze in the conformational landscape of fenchol

E. M. Neeman [a] and T. R. Huet [a,†]

The rotational spectrum of the bicyclic molecule fenchol ($C_{10}H_{18}O$, 1,3,3-trimethylbicyclo[2.2.1]heptan-2-ol) - a biogenic volatile organic coumpound - was recorded in the gas phase using an impulse Fourier transform microwave spectrometer coupled to a supersonic jet expansion over the 2-20 GHz range. Quantum chemical calculations were performed to characterize the conformational landscape of the two diastereoisomers, endo-fenchol and exo-fenchol, with respect to the orientation of the hydroxyl group. The three most stable structures for each diastereoisomer were optimized at the MP2/6-311++G(2df,p) level of theory. Two of them were found to be very close in energy. Molecular parameters obtained from the analysis of observed signals led to the observation of one conformer per diastereoisomer. For the endo-fenchol molecule the r_s geometry associated with the hydroxyl group was obtained, from the observation and analysis of the rotational spectra associated with the deuterated hydroxyl group. The nuclear quadrupolar hyperfine signature was identified. The hydroxyl group was found to be oriented into the direction of the methyl groups attached to C_3, for the more stable conformer of endo-fenchol. For exo-fenchol, it is oriented into the methyl group attached to C_1.

Introduction

The emission of biogenic volatile organic compounds (BVOCs) from plants has strong relevance for plant physiology, plant ecology and atmospheric chemistry.[1] It is well established that BVOCs play a major role in atmospheric chemistry. Besides methane and isoprene, large quantities of monoterpenes are emitted by a variety of plants and coniferous forests are atmospheric pollutants.[2-4] On a global scale, the emissions of BVOCs have been estimated to be 1150 TgC yr^{-1}, of which 11% is attributed to monoterpenes.[5] BVOCs are known to contribute significantly to the formation of secondary organic aerosols (SOAs)[6] and tropospheric ozone.[7-8] The degradation of monoterpenes mostly occurs is due to the reaction with OH radical in the daytime and with NO_3 in night-time. Aerosols play a key role in many environmental processes. Indeed they affect the Earth's radiation balance by scattering the solar radiation and by acting as cloud condensation nuclei. They also participate in heterogeneous chemical reactions in the atmosphere. They finally have considerable effects on health.[9-10] The gas phase structure of a few bicyclic monoterpenes has been experimentally characterized, as α- and β-pinene,[11-12] camphene,[13] camphor,[14] nopinone,[12] and fenchone.[15]

The information on bicyclic alcohol molecules is still very scarce. Fenchol ($C_{10}H_{18}O$, 1,3,3-trimethylbicyclo[2.2.1]heptan-2-ol) also known as fenchyl alcohol, is a bicyclic monoterpene with a hydroxyl group. It has been identified as one of several products emitted from Eucalyptus globulus, Cedrus atlantica,[16] radiata pine wood,[17] particleboard and fibreboard.[18] Finally fenchyl alcohol is considered as flagrance ingredient. The conformational landscape of fenchol is a subject of interest. Indeed there are two diastereoisomer differing by the position of the hydroxyl group, as illustrated in Figure 1. Endo-fenchol has been subject of an NIR-VCD[19] study to explore its chirality, but to our knowledge, there is no experimental information about the orientation of the OH group in the gas phase. Rotational spectroscopy combined with quantum chemical calculations have been proved to be powerful tools to study molecular structure and recognize the observed conformers in the gas phase. Indeed studies have been performed on cyclic alcohols such as 1-methylcyclohexanol,[20] cyclobutanol,[21-22] benzyl alcohol[23] or on the non-cyclic n-propanol[24] in order to identify the orientation and the position of the hydroxyl group.

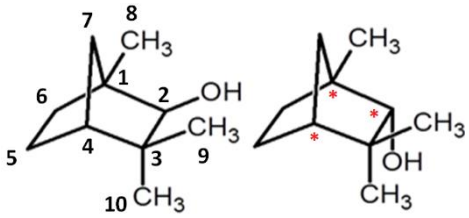

Figure 1. The two diastereoisomers of the 1,3,3-trimethylbicyclo[2.2.1]heptan-2-ol molecule: exo-fenchol (left) and endo-fenchol (right). The carbon atoms are numbered, and the stereogenic centres are indicated by an asterisk.

In this work, we present the conformational study of the fenchol molecule, revealed by impulse Fabry-Pérot Fourier-transform microwave spectroscopy technique coupled to a pulsed molecular expansion (FP-FTMW spectrometer).[25-27] Quantum chemical calculations were performed to identify the more stable conformers of each diastereoisomer, by rotating the hydroxyl group. Moreover in order to identifiy unambiguously the observed structures, we also studied the rotational spectrum of fenchol with the OD functional group. The spectrum was observed for the endo-fenchol molecule. Therefore the rotational constants of the two observed isotopologues have been used to determine the substitution (r_s) geometry of the hydroxyl group.[28-30] The equilibrium related mass-dependence geometry ($r_m^{(1)}$)[31-32] could not be obtained. The molecular parameters associated with the nuclear quadrupole hyperfine structure were compared to the calculated ones. At the end the conformational landscape of fenchol was decrypted thanks to the combination of experimental results supported by high level quantum chemical

calculations. The results presented in this work are of interest to better understand in the future the formation of complexes, namely through rotational, Raman and infrared spectroscopy, and the atmospheric chemistry of fenchol.

Methods

Experimental

The pure rotational spectra (2-20 GHz) of fenchol were recorded using the Fourier transform microwave spectrometer coupled to a supersonic jet expansion in Lille.[33,34] Fenchol (≥ 99% of purity, sum of enantiomers, GC) was purchased from Sigma-Aldrich and used without further purification. The neat solid fenchol was heated in a reservoir in order to be vaporized at 373 K and mixed with neon at a stagnation pressure of 4.5 bars. Then the mixture was introduced into a Fabry-Pérot cavity through a 1 mm diameter pinhole with a pulsed nozzle at a repetition rate of 1.5 Hz. Microwave power pulses of 2 µs duration were used to polarize the molecules which were injected co-axially to the optical axis of the cavity. The Free-Induction Decay (FID) signals were detected at the heterodyne frequency of 30 MHz and digitized at point spacing of 8.33 ns (120 MS/s). FID signals were accumulated, in the low and in the high resolution scan modes in order to obtain a good S/N ratio. After a fast Fourier transformation of the time domain signals, lines were observed as Doppler doublets (~10 kHz full width at half maximum). The central frequency of each line was determined by averaging the frequencies of the two Doppler components, in the high resolution scan mode. The spectral resolution depends on the number of recorded data points, i. e. most of the time a frequency grid of 0.92 and 1.84 kHz was used respectively for the strong and the weak lines, respectively. The quantum number values are limited by the low rotational temperature observed in our molecular beam (a few Kelvin). Because the maximum polarization of the molecule is reached with a π/2 pulse excitation, the amplitude of the electric field was increased or decreased depending on the type of lines, to compensate the lower or higher value of the permanent dipole moment components, respectively. The deuterated species were obtained by direct proton exchange with D_2O.

Quantum chemical calculations

The theoretical calculations were performed using the Gaussian 09, Rev. D.01, software package (G09)[35] and MOLPRO 2015 package of programs.[36] At first the structures of endo- and exo-fenchol were optimized using *ab initio* calculations at the MP2 level of the theory (Møller-Plesset second order perturbation theory) with the Pople split-valence triple-zeta basis set augmented with diffuse and polarization functions on all atoms (the 6-311++G(d,p) basis set).[37-38] Then the potential energy curve associated with the rotation of the OH group was calculated at the MP2/6-311G level, followed for each rotamer by an optimization of the structure at the MP2/6-311++G(d,p), MP2/6-311++G(2df,p), and MP2/aug-cc-pVTZ[39] levels. The molecular parameters and the harmonic force field have been evaluated, with the 6-311++G(d,p) and aug-cc-pVTZ basis sets. In particular the principal rotational constants (A, B, C), and the quartic centrifugal distortion parameters (Δ_J, Δ_{JK}, Δ_K, δ_J, δ_K) of the Watson's Hamiltonian[40] have been calculated for the main species, as well as the electric dipole moment components. Finally for the endo-fenchol molecule, the nuclear quadrupole coupling constants were obtained for the deuterium atom of the deuterated hydroxyl group, at the MP2/aug-cc-pVTZ level of theory, from the equilibrium structure. Additional calculations were performed at the MP2/6-311++G(d,p) level using the r_s geometry. The C1-C2-O-D torsional angle was optimized in order to reproduce the r_s structure of the hydroxyl bond, for the observed conformer.

Results

Theoretical conformational landscape

The conformational landscape calculated along the C1-C2-O-H dihedral angle is presented in Figure 2, for the two diastereoisomers. In each case three rotamers are evidenced within 5 kJ/mol, at the MP2/6-311++G(d,p) level. The less stable rotamer associated with both endo- and exo-fenchol (labelled 3EF and 3XF, respectively) is presenting an OH functional group oriented in the opposite direction of the C2-H bond. The two more stable rotamers associated with the two diastereoisomers (labelled 1EF, 2EF and 1XF, 2XF) are very close in energy, and are separated by a low barrier height, of a few kJ/mol. The OH functional group is oriented in the direction of either the methyl group attached to C1 (1EF, 1XF), or the methyl groups attached to C3 (2EF, 2XF). The equilibrium structure energies calculated with different basis sets are summarized in Table 1.
Interestingly for the exo-fenchol molecule all calculations are in good agreement in terms of relative energy, while for the endo-fenchol molecule the relative stability of the two most stable conformers is not obvious, even when including the zero-point energy correction (ZPE).

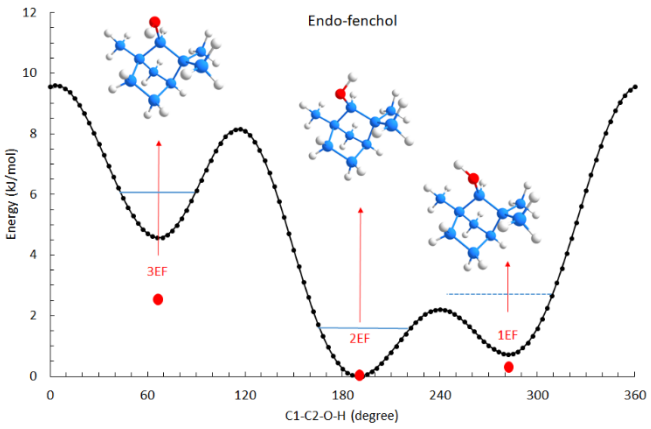

Figure 2. The potential energy curve (MP2/6-311G level) associated with the rotation of the OH functional group for the endo-fenchol (upper) and the exo-fenchol (lower) molecules. The equilibrium position of the three most stable rotamers, calculated at the MP2/6-311++G(2df,p) level, is indicated with red marks. Ground state levels are crudely indicated (see text).

At the best level reached in the present work, the more stable conformers associated with endo-fenchol and exo-fenchol

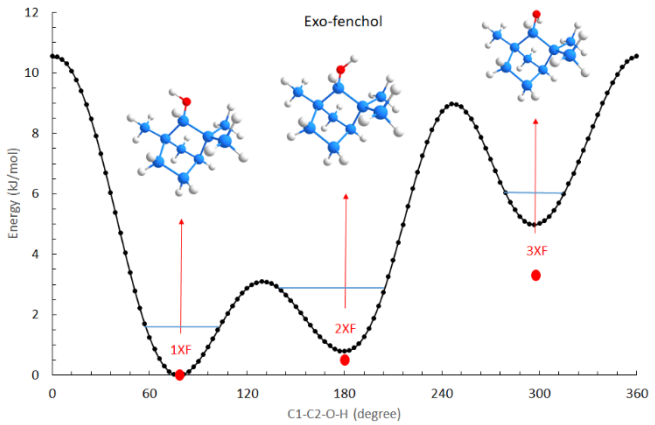

(labelled 2EF and 1XF, respectively) are presenting an OH functional group oriented into the direction of the methyl group(s) attached either to C3 or to C1. However the energy values are so close to those of the 1EF and 2XF conformers that the conclusion is not fully supported due to calculation uncertainties, estimated to be lower than 1 kJ/mol. Structures are detailed in the ESI. Values are reported with respect to each diastereoisomer, but the difference of absolute energy values between the 2EF and 1XF conformers is very low (0.1 kJ/mol), at the MP2/6-311++G(d,p) level with ZPE corrections.

Table 1. Relative energies (kJ/mol) of the three more stable conformers of endo-fenchol and exo-fenchol calculated at the MP2 level of theory with different basis set.

	Endo-fenchol			Exo-fenchol		
MP2/Basis set	1EF	2EF	3EF	1XF	2XF	3XF
6-311G	0.7	0.0	4.5	0.0	0.8	5.0
6-311++G(d,p)[a]	0.03	0.0	2.7	0.0	1.4	4.3
6-311++G(2df,p)	0.2 [a]	0.0 [a]	2.6 [a]	0.0	1.2	3.6
aug-cc-pVTZ	0.0	0.2	2.0	0.0	1.3	3.4

[a] including ZPE correction

Molecular parameters

The experimental rotational spectrum being recorded in a supersonic jet, signals from the 1EF, 2EF, 1XF, and 2XF conformers were initially expected to be observed. A portion of the rotational spectrum, in the scan mode, is shown in Figure 3. By optimizing the temperature in order to minimize the decomposition of fenchol, spectra were left with two series of strong and weak signals. No splitting assignable to a large amplitude motion was observed in the spectrum, even at high resolution. Therefore the observed transitions were fitted to a Watson's Hamiltonian[40] in the A-reduction:

$$H_{rot}^{(A)} = B_x^{(A)} J_x^2 + B_y^{(A)} J_y^2 + B_z^{(A)} J_z^2 - \Delta_J \vec{J}^4 - \Delta_{JK} \vec{J}^2 J_z^2 - \Delta_K J_z^4 - \frac{1}{2}\left[\delta_J \vec{J}^2 + \delta_K J_z^2, J_+^2 - J_-^2\right]_+$$

The I^r representation ($x = b, y = c, z = a$) was used.

For the series of strong lines (labelled E on Figure 3), the lower and the higher microwave polarization power was used to observe a, c-type and b-type transitions, respectively. It means that the dipole moment components are following the relationship $|\mu_a| \cong |\mu_c| \gg |\mu_b|$. More than one hundred lines were measured in the high resolution mode, up to $J = 9$ and $K_a = 6$, and assigned. The SPFIT/SPCAT suite of programs developed by Pickett[41] was used to obtain the molecular parameters. The fitted values of the constants, along with the root mean square value on the line frequencies (RMS) are presented in Table 2. By comparison with the calculated molecular parameters, the strong signals were associated with the endo-fenchol molecule. Because of the very similar values of the calculated A, B, C constants and dipole components, the observed species could be either the 1EF or the 2EF conformer. Meanwhile the value of the asymmetry parameter κ indicates that the observed conformer is 2EF.

In the same way, for the series of weak signals (labelled X on Figure 3), the lower and the higher microwave polarization power was used to observe a-type and b, c-type transitions respectively, which means that $|\mu_a| > |\mu_c| \cong |\mu_b|$. About forty lines were assigned up to $J = 8$ and $K_a = 4$.

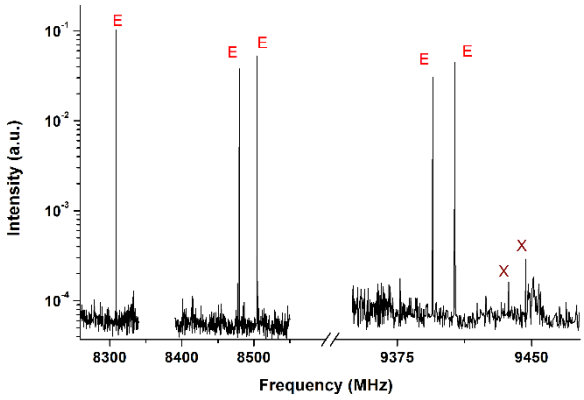

Figure 3. A portion of the microwave spectrum of fenchol showing two series of strong (E) and weak (X) rotational lines. The low resolution scan mode of the impulse FP-FTMW spectrometer was used. Intensity is in arbitrary units.

Table 2. Rotational constants, quartic centrifugal distortion parameters, and dipole moment components for the more stable conformers endo-fenchol and exo-fenchol, determined experimentally from the ground state, and theoretically from the equilibrium structure. The root mean square (RMS) value on the line frequencies and the number of data (N) are also indicated.

		Endo-fenchol			
Constant	Exp.	1EF[a,b]	1EF[a,c]	2EF[a,b]	2EF[a,c]
A/MHz	1520.225823(63)	-0.3%	-0.8%	-0.5%	-1.0%
B/MHz	1097.367672(37)	-1.0%	-1.7%	-0.4%	-1.2%
C/MHz	983.704765(33)	-0.1%	-0.8%	-0.6%	-1.2%
κ^d	-0.576	-0.542	-0.542	-0.581	-0.575
Δ_J/kHz	0.04410(35)	15.8%	-	10.0%	-
Δ_{JK}/kHz	-0.0294(17)	-25.5%	-	-69.0%	-
Δ_K/kHz	0.0567(20)	-3.7%	-	-25.7%	-
δ_J/kHz	0.00626(17)	20.1%	-	15.2%	-
δ_K/kHz	0.1364(26)	42.9%	-	23.4%	-
RMS/kHz	1.5	-	-	-	-
N	114	-	-	-	-
$\lvert\mu_a\rvert$/D	-	1.2	1.1	1.1	1.0
$\lvert\mu_b\rvert$/D	-	0.02	0.03	0.04	0.06
$\lvert\mu_c\rvert$/D	-	1.1	1.1	1.0	0.94
		Exo-fenchol			
Constant	Exp.	1XF[a,b]	1XF[a,c]	2XF[a,b]	2XF[a,c]
A/MHz	1494.88444(30)	-0.4%	-0.9%	-0.5%	-1.1%
B/MHz	1201.81175(13)	-0.6%	-1.3%	-0.8%	-1.4%
C/MHz	901.905933(74)	-0.6%	-1.2%	-0.6%	-1.3%
κ^d	-0.012	-0.019	-0.023	-0.021	-0.023
Δ_J/kHz	0.0285(12)	-69.5%	-	-67.4%	-
Δ_{JK}/kHz	-	-0.0561	-	-0.0572	-
Δ_K/kHz	0.035(14)	33.7%	-	28.0%	-
δ_J/kHz	0.00626(71)	42.5%	-	42.5%	-
δ_K/kHz	-	0.023	-	0.024	-
RMS/kHz	1.2	-	-	-	-
N	42	-	-	-	-
$\lvert\mu_a\rvert$/D	-	1.2	1.0	1.3	1.1
$\lvert\mu_b\rvert$/D	-	0.7	0.6	0.8	0.6
$\lvert\mu_c\rvert$/D	-	0.8	0.7	0.6	0.5

[a] Deviation (%) calculated as (Exp-Theo)/Exp ; [b] MP2/6-311++G(d,p) level ; [c] MP2/aug-cc-pVTZ level ; [d] κ = (2B-A-C)/(A-C).

The fitted molecular parameters are presented in Table 2. All the assigned lines of fenchol are available in the supplementary material, with the SPFIT output files reformatted with the PIFORM program.[42] The observed conformer can be associated with the exo-fenchol molecule. The observed species (κ=-0.012) can be assigned to either the 1XF or the 2XF conformer. In this case, 1XF conformer is more stable than 2XF by about 1.3 kJ/mol. Therefore we can assign the observed transitions to the 1XF rotamer. As recently reported in the high-resolution spectroscopic study of

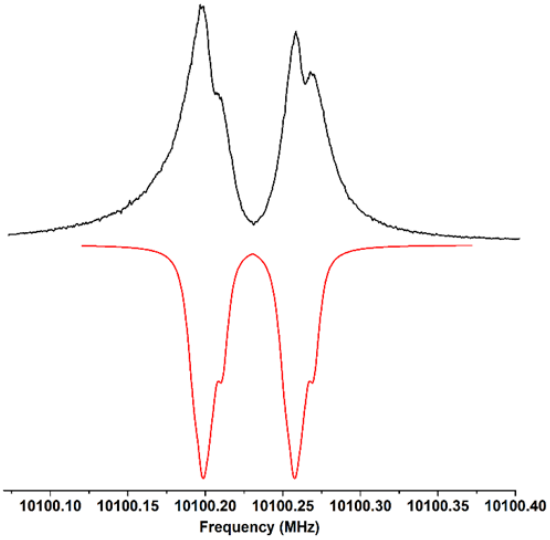

Figure 4. Experimental (black) and simulated (red) hyperfine structure associated with the $J_{KaKc} = 4_{23} - 3_{13}$ rotational line for the observed conformer of endo-fenchol. A Lorentzian line shape with a full width at half maximum of 7.0 kHz was adjusted on each hyperfine component.

camphene,[13] β-pinene and nopinone,[12] a few rotational lines of fenchol also display complex line-shapes with several components of various intensities separated by a few tens of kHz that do not arise from the methyl group torsion. Indeed the internal rotation of the methyl groups was not observed, as in any of the previously cited molecules, due to the high calculated barrier height. Each complex line-shape is associated with the magnetic interaction between close nuclear hydrogen spins. It was shown that the hyperfine structure could be well modelled by only considering the pairs of hydrogen atoms from the three $(-CH_2-)$ methylene. The hyperfine geometrical parameters were evaluated using the MP2/aug-cc-pVTZ structure. Indeed for two nuclear spins denoted $\boldsymbol{I_1}$ and $\boldsymbol{I_2}$, the nuclear spin-spin Hamiltonian can be written as:[43-44]

$$H_{nss} = \boldsymbol{I_1}.\boldsymbol{D}.\boldsymbol{I_2}$$

in which the second-rank direct dipolar spin-spin coupling tensor $\boldsymbol{D}$ contains information about the inter-nuclear vectors. The tensor elements are defined by

$$D_{ij}^{12} = g_1 g_2 \frac{\mu_0 \mu_N^2}{4\pi} \frac{R^2 \delta_{ij} - 3\boldsymbol{R_i}\boldsymbol{R_j}}{R^5} \beta$$

g_1 and g_2 are the nuclear g factors for nuclei 1 and 2, μ_N is the nuclear magneton, $\boldsymbol{R_i}$ and $\boldsymbol{R_j}$ are the position vectors of nuclei in the principal inertial axis system, with $i, j = a, b, c$ and R is the length of the vector joining the two nuclei. The associated line shapes were simulated using the SPCAT program[41], with a Lorentz profile adjusted on each calculated hyperfine component. As illustrated in Figure 4 for endo-fenchol, a good agreement is observed on both the frequency and intensity scales.

Deuteration of the hydroxyl group

The comparison of the experimental molecular parameters values to the theoretical ones is not obvious, due to the low mass of hydrogen in OH (see Table 2). Therefore we recorded the rotational spectrum of fenchol with the hydroxyl group deuterated. The molecular parameters were calculated from the equilibrium structures presented in Figure 2, at the MP2/6-311++G(d,p) level of theory. A set of 52 rotational lines was observed for endo-fenchol, up to $J = 10$ and $K_a = 4$. The signature of the nuclear quadrupole interaction effect for the deuterium nucleus was clearly resolved on several lines, as displayed on Figure 5. The nuclear quadrupole interaction term[45] is written as:

$$H_Q^{(D)} = \frac{1}{6} \sum_{i,j=x,y,z} Q_{ij}^{(D)} V_{ij}^{(D)}$$

Figure 5. Experimental quadrupole splitting associated with the $J_{KaKc} = 4_{13} - 3_{13}$ line for the most stable conformer of endo-fenchol, with a deuterated hydroxyl group. The lines are assigned with the F quantum number. The F=3-2 signal is hidden by the strong F=5-4 line.

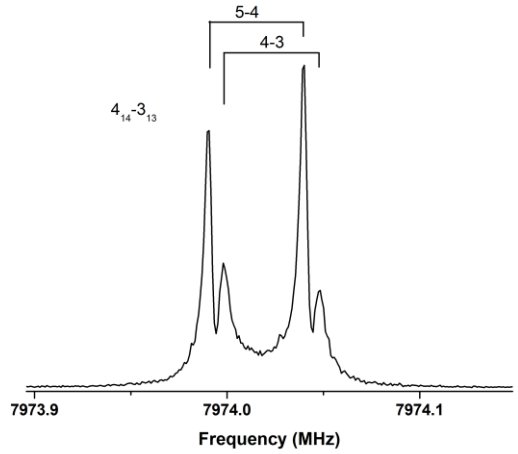

Table 3. Rotational constants, quartic centrifugal distortion parameters, and nuclear quadrupole constants for the more stable conformer of endo-fenchol, with an OD functional group, determined experimentally from the ground state, and theoretically from the equilibrium structure. The root mean square (RMS) value on the line frequencies and the number of data (N) are also indicated.

Constant	Exp.	1EF[a,b]	2EF[a,b]	1EF[a,c]	2EF[a,c]
A/MHz	1488.66758(24)	-0.8%	-1.1%	-0.7%	-0.9%
B/MHz	1094.44232(19)	-1.3%	-1.4%	-1.8%	-1.3%
C/MHz	971.07906(12)	-0.4%	-1.2%	-0.7%	-1.1%
κ[d]	-0.523	-0.480	-0.514	-0.487	-0.514
Δ_J/kHz	0.0486(11)	-	-	-	-
Δ_{JK}/kHz	-0.015(11)	-	-	-	-
Δ_K/kHz	0.035(12)	-	-	-	-
δ_J/kHz	0.00698(93)	-	-	-	-
δ_K/kHz	0.161(17)	-	-	-	-
$1.5\chi_{aa}$/MHz	0.0941(80)	0.1491[e]	0.1091[e]	0.1210	0.1201
$(\chi_{bb}-\chi_{cc})/4$/MHz	0.0719(38)	0.0454[e]	0.0588[e]	0.0482	0.0594
RMS/kHz	2.6	-	-	-	-
N	144	-	-	-	-

[a] Deviation (%) calculated as (Exp-Theo)/Exp ; [b] MP2/6-311++G(d,p) level of theory; [c] MP2/aug-cc-pVTZ level of theory at the equilibrium structure ; [d] κ = (2B-A-C)/(A-C) ; [e] MP2/6-311++G(d,p) level using the r_s coordinate of the D atom.

Table 4. Coordinates (a, b, c) in Å for the hydrogen or deuterium atom of the hydroxyl group, for the endo-fenchol molecule.

	a	b	c
Calculated 2EF[a]	0.541	-2.592	-0.731
Calculated 1EF[a]	-0.635	-2.604	-0.651
Experimental (r_s)	±0.6394(24)	±2.4853(6)	±0.9463(16)

[a] MP2/aug-cc-pVTZ level.

This equation describes the interaction between the nuclear quadrupole electric moment $Q^{(D)}$ and the molecular electric field gradient $V^{(D)}$ for the deuterium nucleus.The spectroscopic parameters are the elements of the quadrupole coupling tensor given by:

$$\chi_{\alpha\beta}^{(D)} = eQ^{(D)} \frac{\partial^2 V^{(D)}}{\partial\alpha\partial\beta}$$

α and β refer to the coordinates a, b, c in the principal inertial axes and e denotes the elementary charge. The fitted values of the constants, along with the root mean square value on the line frequencies (RMS) are presented in Table 3. Again, the value of the asymmetry parameter is in favor of the 2EF rotamer.

Moreover, compared with the calculated values at the MP2/aug-cc-PVTZ level, the observed value of the quadrupole constant χ_{ii} are significantly different in the 1EF and 2EF conformers (Table 3, columns 2, 5, 6). The observed value of χ_{ii} is in better agreement with the value calculated for the 2EF conformer. Meanwhile with about 30% of discrepancies, the calculated χ_{ii} values are still far from the observed ones. We

should note that due to the small intensity of the exo-fenchol signals, the observation of the OD form was not possible.

Experimental structure of the hydroxyl group

The results presented in this section have been obtained by using the computer programs STRFIT and KRA.[42] The two sets of experimental rotational constants obtained for endo-fenchol were used together to determine the position and the orientation of the hydroxyl group. The r_s structure based on Kraitchman's equations was used,[28] with the uncertainties from vibration-rotation effects as estimated by Costain.[29] The obtained result is reported in Table 4. The values of the calculated and experimental coordinates can be compared. Unfortunately the position calculated for the hydrogen or deuterium atom, in the 1EF and 2EF rotamers, is mainly differing by the sign of the a coordinate, while the r_s structure is only giving its absolute value. However, by considering the two sets of possible signs, the semi-experimental OH length was calculated. A value of 0.972 Å and 0.883 Å was obtained for the 2EF and 1EF conformers, respectively, to be compared with a calculated bond length of OH equal to 0.964 Å. Clearly the OH bond length associated with the 1EF conformer is not possible. At the same time the result obtained for the 2EF conformer is quite good. Then by freezing the obtained coordinates of the hydrogen atom of the OH group and optimizing the structure of both rotamers we obtained new semi-experimental nuclear quadrupole constants for deuterium, using the *ab initio* MP2/6-311++G(d,p) calculation (Table 3, columns 2, 3, 4). The values obtained for the 2EF rotamer fit well the experimental values. Finally the $|\mu_b|$ dipole moment value for the 2EF conformer is updated to 0.08D, in good agreement with the small b-type transitions observed in the spectra, while for the 1EF rotamer it is decreased to 0.01D.

Discussion

The conformational landscape of fenchol

The experimental and theoretical results obtained in the present study are rationalized hereafter. At first we rely on *ab initio* calculations to say that the more stable conformers of both diastereoisomers are very close, nearly degenerate, in energy. Indeed the fact that the observed rotational lines associated with endo-fenchol are more intense (by two orders of magnitude) than those of exo-fenchol can be explained by the almost enantiopure (1R)-endo-(+)-fenchol composition of the available commercial samples.

If three rotamers were calculated within 5 kJ/mol for each diastereoisomer, only one rotamer was observed in each case. The supersonic molecular expansion used in this work is favouring the population of conformers 1 and 2, and not of conformer 3. In addition, because of the low barrier height between conformers 1 and 2 in both diastereoisomers, relaxation to the more stable conformer is possible. It has been reported that for low barrier height less than 4.7 kJ/mol (≈400 cm-1)[46] the relaxation is observed for several molecules. We also observed it, namely for limonene and carvone.[47] In fenchol, the relaxation process can be illustrated by calculating the ground state (GS) energies on the potential curve of Figure 2. It was crudely estimated by taking ½ of the imaginary frequency of the corresponding transition state. The result is the following: GS(3EF) = 1.36 kJ/mol, GS(2EF) = 1.69 kJ/mol, GS(1EF) = 2.00 kJ/mol. The GS(1EF) being about 0.52 kJ/mol above the transition state, it is not stable. Thus, according to this qualitative model, one does expect to observe only one conformer (2EF), to be modeled with a semi-rigid rotor Hamiltonian. Consequently, we are left with only one populated conformer, probed by the microwave radiation in the supersonic jet, for each diastereoisomer.

The two conformers observed in the gas phase are the 2EF and 1XF rotamers of endo- and exo-fenchol, respectively. Indeed the two sets of experimental rotational constants (A, B, C) indicate that the signals are associated with the two diastereoisomers. Then the *ab initio* calculations, performed at the MP2/6-311++G(2df,p) and MP2/aug-cc-pVTZ levels, are predicting the structures 2EF and 1XF as being the more stable, but very close in energy with the 1EF and 2XF rotamers.

For endo-fenchol the deuteration of the hydroxyl group was giving access to the quadrupole hyperfine structure for the endo-fenchol rotamer, and to the r_s coordinates of the D atom. On the one hand the spectrum is identified to the 2EF rotamer thanks to the fingerprint signature associated with the value of the χ_{ii} constants. On the other hand the semi-experimental bond length of the hydroxyl group can unambiguously only be associated with the 2EF rotamer. It should be mentioned that this geometry reproduces at best the asymmetry parameter coming from experimental constants. Therefore for endo-fenchol, the hydroxyl group is oriented into the direction of the two methyl groups attached to C3.

Even if the calculated conformational landscapes of the two diastereisomers are very comparable, the 1XF rotamer is calculated to be unambiguously the most stable one for exo-fenchol. Unfortunately the experimental molecular parameters do not provide further information. Consequently, we can reasonably suggest that the 1XF rotamer is the most stable conformer for exo-fenchol, *i. e.* the hydroxyl group is oriented into the direction of the methyl group attached to C1.

Finally it is shown in the present bicyclic alcohol that the hydroxyl group is attached to an aliphatic carbon atom. It can rotate along the C–O bond, connecting three non-equivalent energy minima in each of the two diastereoisomers. It should be noted that if the transition states are separated by 120°, it is not the case of the minima. Indeed for endo-fenchol, the minima are located at 66°, 189°, and 282° (see Fig. 2). They are therefore separated by 123°, 93°, and 144°. The slightly higher stability of the 2EF and 1XF rotamers versus the 1EF and 2XF rotamers is probably related to the higher distance of the hydroxyl hydrogen with respect to the surrounding hydrogen atoms.

The hydroxyl structure in a bicyclic alcohol

The results obtained for a bicyclic alcohol such as 1,3,3-trimethylbicyclo[2.2.1]heptan-2-ol (fenchol) are discussed on

view of a few literature results on cyclic alcohols such as 1-methylcyclohexanol,[20] cyclobutanol,[21-22] benzyl alcohol[23] or on the non-cyclic n-propanol.[24]

In non-cyclic structures, rotational spectroscopy combined to chemistry quantum chemistry calculations has revealed the structures of several conformers, and the observation of tunneling splitting due to the internal rotation of the hydroxyl group. [24] In cyclic structures, the number of conformers might be reduced, but the chemical physics is related to the same problems. [20-23]

To our knowledge, there are no detailed study for bicyclic alcohol. The most striking feature in fenchol is the fact that all the rotamers exhibit non-equivalent structures, and no tunneling motion characterized by splitting. Meanwhile the fact that the torsional angle associated with the hydroxyl group could be adjusted in order to reproduce experimental data, is an indication that characterizing bicyclic alcohol structures with accuracy is becoming possible.

Conclusion

The conformational landscape of fenchol, a bicyclic alcohol, has been characterized by using *ab initio* calculations and microwave spectroscopy. The position of the hydroxyl group was evidenced in the two diastereoisomers. The equilibrium structure of three rotamers was calculated within 5 kJ/mol, for each molecule. Only the most stable rotamer was observed in a supersonic molecular jet probed by impulse microwave radiation. The high resolution spectroscopic technique employed allowed the identification of the two rotamers as being these with the hydroxyl group oriented into the direction of the methyl group attached to C1 for exo-fenchol, and into the direction of the two methyl groups attached to C3 for endo-fenchol.

Fenchol being a natural molecule emitted into the atmosphere, it is expected to react and to form molecular complexes. The fact that the two stable rotamers of both endo- and exo-fenchol are only separated by a barrier height of a few kJ/mol is of interest for further investigations related to molecular dynamics.

Acknowledgements

The present work was funded by the French ANR *Labex CaPPA* through the PIA under contract ANR-11-LABX-0005-01, by the Regional Council *Hauts-de-France* and by the European Funds for Regional Economic Development (FEDER). It is a contribution to the scientific project CPER CLIMIBIO. T. R. Huet acknowledges M. Suhm for fruitful exchanges.

The authors declare no conflict of interest.

References

1 R. Baraldi, F. Rapparini, O. Facini, D. Spano and P. Duce, *Journal of Mediterranean Ecology*, 2005, **6**, 3-9.
2 F.M.N. Nunes, M.C.C. Veloso, P.A. de P. Pereira, J.B. de Andrade, *Atmospheric Environment,* 2005, **39**, 7715.
3 A. Calogirou, B.R. Larsen, D. Kotzias, *Atmospheric Environment,* 1999, **33**, 1423.
4 F. Chiron, J.C. Chalchat, R.P. Garry, J.F. Pilichowski, J. Lacoste, *J. Photochem. Photobiol. A: Chem.,* 1997, **111**, 75.
5 B. C. Singer, B. K. Coleman, H. Destaillats, A. T. Hodgson, M. M. Lunden, C. J. Weschler, W. W. Nazaroff, *Atmospheric Environment,* 2006, **40**, 6696−6710.
6 L. V. Rizzo, P. Artaxo, T. Karl, A. B. Guenther, J. Greenberg, *Atmospheric Environment,* 2010, **44**, 503−511.
7 T. Hoffmann, J. R. Odum, F. Bowman, D. Collins, D. Klockow, R. C. Flagan, J. H. Seinfeld, *J. Atmos. Chem.,* 1997, **26**, 189−222.
8 D. Kotzias, J. L. Hjorth, H. Skov, *Toxicol. Environ. Chem.,* 1989, **20–21**, 95−99.
9 J. Lelieveld, T. M. Butler, J. N. Crowley, T. J. Dillon, H. Fischer, L. Ganzeveld, H. Harder, M. G. Lawrence, M. Martinez, D. Taraborrelli and J. Williams, *Nature,* 2008, **452** 737-740.
10 M. Hallquist, J. C.Wenger, U. Baltensperger, Y. Rudich, D. Simpson, M. Claeys, J. Dommen, N. M. Donahue, C. George, A. H. Goldstein, J. F. Hamilton, H. Herrmann, T. Hoffmann, Y. Iinuma, M. Jang, M. E. Jenkin, J. L. Jimenez, A. Kiendler-Scharr, W. Maenhaut, G. McFiggans, Th. F. Mentel, A. Monod, A. S. H. Prévôt, J. H. Seinfeld, J. D. Surratt, R. Szmigielski, and J. Wildt, *Atmos. Chem. Phys.,* 2009, **9**, 5155–5236.
11 E. M. Neeman, J. R. Aviles Moreno, and T. R. Huet, *J. Chem. Phys.*, 2017, **147**, 214305.
12 E. M. Neeman, J. R. Aviles Moreno, and T. R. Huet, *Phys. Chem. Chem. Phys.*, 2017, **19**, 13819-13827.
13 E. M. Neeman, P. Dréan and T. R. Huet, *J. Mol. Spectrosc.*, 2016, **322**, 50.
14 Z. Kisiel, O. Desyatnyk, E. Bialkowska-Jaworska and L. Pszczólkowski, *Phys. Chem. Chem. Phys.*, 2003, **5**, 820.
15 D. Loru, M. A. Bermúdez, and M. E. Sanz, *J. Chem. Phys.*, 2016, 145, 074311.
16 N. Yassaa, B. Y. Meklati, A. Cecinato, *Atmospheric Environment*, 2000, **34**, 2809-2816
17 A. G. McDonald, J. S. Gifford, D. Steward, P. H. Dare, S. Riley and I. Simpson, *Holz Roh Werkst.* 2004, **62**, 291–302
18 M. G.D. Baumann, L. F. Lorenz, S. A. Batterman, G.-Z. Zhang. *Forest Products Journal*, 2000, **50**, no. 9, 75-82.
19 S. Abbate, E. Castiglioni, F. Gangemi, R. Gangemi, and G. Longhi, *Chirality*, 2009, ***21*(1E)**, E242-E252.
20 W. Li, L. Spada, L. Evangelisti and W. Caminati, *The Journal of Physical Chemistry A*, 2016, **120**, 4338-4342.
21 J. N. Macdonald, D. Norbury and J. Sheridan, *Spectrochimica Acta Part A: Molecular Spectroscopy,* 1978, **34**, 815-818.
22 W. Lin, A. Ganguly, A. J. Minei, G. L. Lindeke, W. C. Pringle, S. E. Novick, and J. R. Durig, *Journal of Molecular Structure*, 2009, **922**, 83-87.
23 K. A. Utzat, R. K. Bohn, J. A. Montgomery Jr, H. H. Michels, and W. Caminati, *The Journal of Physical Chemistry A*, 2010, **114**, 6913-6916.
24 Z. Kisiel, O. Dorosh, A. Maeda, I. R. Medvedev, F. C. De Lucia, E. Herbst, B. J. Drouin, J. C. Pearson and S. T. Shipmand, *Phys. Chem. Chem. Phys.*, 2010, **12,** 8329–8339.
25 T. J. Balle and W. H. Flygare, *Rev. Sci. Instrum.*, 1981, **52(1)**, 33.
26 J.-U. Grabow, W. Stahl, H. Dreizler, *Rev. Sci. Instrum.*, 1996, **67(12)**, 4072.
27 J.-U. Grabow, in *Handbook of high-resolution spectroscopy*, Vol 2, M. Quack and F. Merkt Ed., Wiley 2011.
28 J. Kraitchman, *Am. J. Phys.*, 1953, **21**, 17.
29 C. C. Constain, *Trans. Am. Crystallogr. Assoc.*, 1966, **2**, 157.
30 H. D. Rudolph and J. Demaison, in *Equilibrium Molecular Structures: From Spectroscopy to Quantum Chemistry*, J. Demaison, J.E. Boggs and A.G. Császár, Ed., CRC Press 2010, p. 125-158.
31 J. K. G. Watson, *J. Mol. Spectrosc.*, 1973, **48(3)**, 479.

32 J. K. G. Watson, A. Roytburg, W. Ulrich, *J. Mol. Spectrosc.*, 1999, **196**, 102.
33 S. Kassi, PhD thesis, University of Lille (2000).
34 M. Tudorie, L. H. Coudert, T. R. Huet, D. Jegouso and G. Sedes, J. Chem. Phys. 2011, **134**, 074314.
35 Gaussian 09, Revision D.01, M. J. Frisch, G. W. Trucks, H. B. Schlegel, G. E. Scuseria, M. A. Robb, J. R. Cheeseman, G. Scalmani, V. Barone, B. Mennucci, G. A. Petersson, H. Nakatsuji, M. Caricato, X. Li, H. P. Hratchian, A. F. Izmaylov, J. Bloino, G. Zheng, J. L. Sonnenberg, M. Hada, M. Ehara, K. Toyota, R. Fukuda, J. Hasegawa, M. Ishida, T. Nakajima, Y. Honda, O. Kitao, H. Nakai, T. Vreven, J. A. Montgomery, Jr., J. E. Peralta, F. Ogliaro, M. Bearpark, J. J. Heyd, E. Brothers, K. N. Kudin, V. N. Staroverov, T. Keith, R. Kobayashi, J. Normand, K. Raghavachari, A. Rendell, J. C. Burant, S. S. Iyengar, J. Tomasi, M. Cossi, N. Rega, J. M. Millam, M. Klene, J. E. Knox, J. B. Cross, V. Bakken, C. Adamo, J. Jaramillo, R. Gomperts, R. E. Stratmann, O. Yazyev, A. J. Austin, R. Cammi, C. Pomelli, J. W. Ochterski, R. L. Martin, K. Morokuma, V. G. Zakrzewski, G. A. Voth, P. Salvador, J. J. Dannenberg, S. Dapprich, A. D. Daniels, O. Farkas, J. B. Foresman, J. V. Ortiz, J. Cioslowski, and D. J. Fox, Gaussian, Inc., Wallingford CT, 2013.
36 MOLPRO, version 2015.1, a package of ab initio programs, H.-J. Werner, P. J. Knowles, R. Lindh, F. R. Manby, M. Schütz and others, see http://www.molpro.net.
37 C. Møller, M. S. Plesset, *Phys. Rev.*, 1934, **46**, 618-622.
38 L. A. Curtiss, K. Raghavachari, P. C. Redfern, V. Rassolov, J. A. Pople, *J. Chem. Phys.*, 1998, **109**, 7764.
39 T. H. Dunning Jr, *J. Chem. Phys.*, 1989, **90**, 1007-1023.
40 J. K. G. Watson, in Vibrational Spectra and Structure, J. R. Durig, Ed., Elsevier, Amsterdam, 1977, **6**, 1-87
41 H. M. Pickett, *J. Mol. Spectrosc.*, 1991, **148**, 371-377.
42 Z. Kisiel, in J. Demaison et al (Eds.), Spectroscopy from Space, Kluwer Academic Publishers, Dordrecht (2001) 91-106; PROSPE – Programs for ROtational SPEctroscopy, Institute of Physics, Academy of Science, Warsaw, http://www.ifpan.edu.pl/~kisiel/prospe.htm.
43 P. Thaddeus, L.C. Krisher, J.H.N. Loubster, *J. Chem. Phys.*, 1964, **40**, 257.
44 A. Carrington, J.M. Brown, Rotational Spectroscopy of Diatomic Molecules, Cambridge University Press, Cambridge, **2003**
45 W. Gordy, R. L. Cook, Microwave Molecular Spectra, Wiley: New York, 1984.
46 R. S. Ruoff, T. D. Klots, T. Emilsson, H. S. Gutowsky, *J. Chem. Phys.* 1990, **93**, 3142.
47 J. R. Avilés Moreno, T. R. Huet, and J. J. López González, *Structural Chemistry*, 2013, **24**, 1163-1170.